OPEN

npg

ORIGINAL ARTICLE

Phosphoproteomic analysis identifies activated MET-axis PI3K/AKT and MAPK/ERK in lapatinib-resistant cancer cell line

Yong Yook Lee[1,2,5], Hwang-Phill Kim[3,5], Min Jueng Kang[1,5], Byoung-Kyu Cho[1], Sae-Won Han[4], Tae-You Kim[3,4] and Eugene C Yi[1,2]

Lapatinib, a dual inhibitor of epidermal growth factor receptor (EGFR) and human epidermal growth factor receptor 2 (HER2) tyrosine kinases, has shown promising results as a growth inhibitor of HER2-positive cancer cells *in vitro*. However, similar to other EGFR-targeting drugs, acquired resistance to lapatinib by HER2-positive cancer cells remains a major clinical challenge. To elucidate resistance mechanisms to EGFR/HER2-targeting agents, we performed a systematic quantitative comparison of the phosphoproteome of lapatinib-resistant (LR) human gastric cancer cells (SNU216-LR) versus parental cells (SNU216) using a titanium dioxide (TiO$_2$) phosphopeptide enrichment method and analysis with a Q-Exactive hybrid quadrupole-Orbitrap mass spectrometer. Biological network analysis of differentially expressed phosphoproteins revealed apparent constitutive activation of the MET-axis phosphatidylinositide 3-kinase (PI3K)/α-serine/threonine-protein kinase (AKT) and mitogen-activated protein kinase (MAPK)/extracellular signal-regulated kinase (ERK) signaling pathways in SNU216-LR. Inhibition of the PI3K/AKT and MAPK/ERK signaling pathways in SNU216-LR also leads to cell cycle arrest, confirming the biological network analysis. Lapatinib sensitivity was restored when cells were treated with several molecular targeting agents in combination with lapatinib. Thus, by integrating phosphoproteomic data, protein networks and effects of signaling pathway modulation on cell proliferation, we found that SNU216-LR maintains constitutive activation of the PI3K/AKT and MAPK/ERK pathways in a MET-dependent manner. These findings suggest that pathway activation is a key compensatory intracellular phospho-signaling event that may govern gastric cancer cell resistance to drug treatment.

Experimental & Molecular Medicine (2013) **45**, e64; doi:10.1038/emm.2013.115; published online 22 November 2013

Keywords: drug resistance; HER2-positive gastric cancer; lapatinib; phosphoproteins; Q-Exactive; therapeutic targets

INTRODUCTION

Human epidermal growth factor receptor 2 (HER2) is one of the receptor tyrosine kinases activated through dimerization with members of the epidermal growth factor receptor (EGFR) family.[1] Overexpression of HER2 leads to tumor progression via intracellular signal transduction cascades[2] and is observed in ∼20−30% of high-risk breast cancer cases,[3,4] as well as in 6−35% of invasive gastric cancers.[5] Lapatinib inhibits the proliferation of cancer cells overexpressing EGFR and/or HER2

both *in vitro* and *in vivo*, and it was approved by the United States Food and Drug Administration as a treatment for advanced HER2-positive breast cancer in 2007.[6–8] The antitumor activity of lapatinib has also been examined in gastric cancer cells.[9,10] A phase III clinical trial comparing the effect of chemotherapy alone versus in combination with lapatinib in HER2-positive gastric cancer patients is currently on-going.[11] However, acquired resistance to lapatinib has been and remains a limitation to its therapeutic use in the

clinic because of a poor understanding of the underlying mechanisms.

One possible mechanism driving therapeutic resistance is the compensatory activation of an alternate receptor tyrosine kinase that would restore the downstream signaling pathways.[12,13] Many functional studies of cancers coexpressing hepatocyte growth factor receptor (MET) and EGFR have suggested that compensatory activation of MET in the presence of EGFR blockade may be responsible for EGFR tyrosine kinase inhibitor (TKI)-acquired resistance. For example, Engelman et al.[14] detected MET amplification in patients with non-small-cell lung cancer who developed clinical resistance to the EGFR inhibitors gefitinib or erlotinib.[14] Yano et al.[15] also found that hepatocyte growth factor-mediated MET activation is a novel mechanism of gefitinib resistance in lung adenocarcinomas containing EGFR-activating mutations. These studies imply that the functional cross-talk between MET and the EGFR family of receptor tyrosine kinases plays an important role in the adaptive cellular response that may contribute to drug resistance. More recently, the activation of MET has been shown to confer resistance to lapatinib inhibition in HER2-positive gastric cancer cells.[16]

To identify the affected global cellular processes compensating for the selective pressure of lapatinib on EGFR/HER2, we performed a large-scale quantitative phosphoproteome analysis of lapatinib-resistant (LR) human gastric cancer cells generated from HER2-amplified gastric cancer cells during prolonged lapatinib treatment. By integrating differentially expressed phosphoproteins into the biological network analysis tools, we found that constitutive activation of the phosphatidylinositide 3-kinase (PI3K)/α-serine/threonine-protein kinase (AKT) and mitogen-activated protein kinase (MAPK)/extracellular signal-regulated kinase (ERK) signaling pathways induced by the MET axis may be a critical pathway conferring acquired lapatinib resistance. The phosphoproteomic results were confirmed by cell growth inhibition studies with a single or several molecular targeting agents in combination with lapatinib. These findings provide novel insights into adaptive changes in phospho-signaling networks that occur during the development of lapatinib resistance in human HER2-positive gastric cancer cells. Our data also demonstrate that network-based global phosphoproteomic analysis is a reliable approach for predicting cellular signaling events, which in turn can lead to the identification of alternative targeting strategies for LR gastric cancer.

MATERIALS AND METHODS

Cell lines and reagents

Human gastric carcinoma SNU216 cells were obtained from the Seoul National University Cell Bank (Seoul, Korea). Cells were cultured in RPMI-1640 medium containing 10% (v/v) fetal bovine serum (Gibco, Carlsbad, CA, USA) at 37 °C under 5% CO_2. Lapatinib was a gift from GlaxoSmithKline (Research Triangle Park, NC, USA). NVP-BEZ235, selumetinib, saracatinib and crizotinib were purchased from Selleck Chemicals (Houston, TX, USA). Stock solutions were prepared in dimethyl sulfoxide and stored at −20 °C. Ammonium bicarbonate, dithiothreitol (DTT), formic acid (FA) and trifluoroacetic acid (TFA) were purchased from Sigma-Aldrich (St Louis, MO, USA). The HPLC-grade acetonitrile (ACN) and water were from JT Baker (Phillipsburg, NJ, USA). Lyophilized trypsins were obtained from Promega (Madison, WI, USA).

Generation of LR clones from SNU216 cells in vitro

SNU216 cells were exposed to increasing concentrations of lapatinib over a period of 8 months, reaching a final concentration of 10 μM at the end of this period. Single-cell cloning was done by serial dilution or isolation with cloning cylinders, and isolated resistant cells were expanded in culture medium containing 1 μM lapatinib.

Cell growth inhibition assay

The viability of cells was assessed using MTT assays (Sigma-Aldrich). A total of 3×10^3 cells were seeded in 96-well plates, incubated at 37 °C for 24 h for recovery and treated for 72 h with specific drugs as indicated. After treatment, MTT solution was added to each well followed by incubation for 4 h at 37 °C. The medium was removed, dimethyl sulfoxide was added and the samples were mixed thoroughly for 30 min at room temperature. Cell viability was determined by measuring absorbance at 540 nm using a VersaMax microplate reader (Molecular Devices, Sunnyvale, CA, USA).

Immunoblot analysis

Antibodies against p-EGFR (pY1068), p-HER2 (pY1221/1222), p-MET (pY1234/1235), p-AKT (pS473), p-MAPK (pY202/pY204), p-SRC (pY416), p-RAF (pS338), EGFR, HER2, MET, AKT, MAPK, SRC (proto-oncogene tyrosine-protein kinase Src) and RAF were purchased from Cell Signaling Technology (Beverley, MA, USA). Antibodies directed against β-catenin, cyclin D and p27 were obtained from Santa Cruz Biotechnology (Santa Cruz, CA, USA). Subconfluent cells (70−80%) were used for protein analyses. For the analysis of signaling after drug treatments, cells were treated with different concentrations of the indicated drugs for 48 h. Cell lysates were prepared with RIPA buffer, consisting of 50 mM Tris-HCl (pH 7.5), 1% (v/v) NP-40, 0.1% (w/v) sodium deoxycholate, 150 mM NaCl, 50 mM NaF, 1 mM sodium pyrophosphate, 1 mM sodium vanadate, 1 mM nitrophenylphosphate, 1 mM benzamidine, 0.1 mM PMSF, 0.1 mM aprotinin, 0.1 mM leupeptin and 0.1 mM pepstatin A, on ice for 10 min, after which the lysates were centrifuged at $14\,000 \times g$ for 20 min. Samples containing equal amounts of protein were resolved by sodium dodecyl sulfate-polyacrylamide gel electrophoresis (SDS-PAGE) followed by transfer of the proteins onto nitrocellulose membranes. The membranes were blocked for 1 h at room temperature with 5% (w/v) skim milk and incubated overnight at 4 °C with primary antibody. After probing with secondary antibody for 1 h at room temperature, detection was performed using an enhanced chemiluminescence system (Amersham Pharmacia Biotech, Piscataway, NJ, USA).

Cell cycle analysis

Cells were washed twice in phosphate-buffered saline, fixed in 70% (v/v) ethanol and stored at −20 °C until analysis was performed. Before analysis, thawed cell suspensions were washed with phosphate-buffered saline, digested with RNase A (50 μg ml^{-1}) for 15 min at 37 °C and stained with propidium iodide (50 μg ml^{-1}). The DNA content (10 000 cells per experimental group) was determined using a FACSCalibur flow cytometer (Becton Dickinson Biosciences, San Jose,

CA, USA) equipped with a ModFit LT program (Verity Software House, Topsham, ME, USA), as previously described.[10]

One-dimensional SDS-PAGE fractionation and in-gel digestion

Cells were lysed by sonication in lysis buffer, consisting of 1% (w/v) sodium deoxycholate, 6 M urea, 50 mM Tris-HCl (pH 7.5), 150 mM NaCl, 5 mM EDTA, 50 mM NaF, 1 mM sodium orthovanadate, 0.5 mM PMSF and phosphatase and protease inhibitor (Roche, Mannheim, Germany). Protein concentration was determined using the Micro BCA Protein Assay Kit (Thermo Scientific, Rockford, IL, USA). Protein samples (3 mg each) were dissolved in NuPAGE LDS sample buffer (Invitrogen, Carlsbad, CA, USA) containing 50 mM DTT and heated at 70 °C for 10 min. The cell lysates were separated on a 4−12% Bis-Tris NuPAGE gel (Invitrogen) and stained with Coomassie Brilliant Blue (Sigma-Aldrich). The entire gel lane was cut into six pieces and subjected to in-gel tryptic digestion.[17] The excised gels were destained with 50% (v/v) ACN in 25 mM NH_4HCO_3 and in 100 mM NH_4HCO_3 for 15 min. After destaining, the gels were dried and reduced with 20 mM DTT at 60 °C for 1 h. They were alkylated with 55 mM iodoacetamide at room temperature for 45 min in the dark. The gel pieces were dehydrated for 15 min in 50% ACN in 25 mM NH_4HCO_3, and the proteins in the gels were digested overnight at 37 °C with 13 ng μl^{-1} sequencing-grade modified trypsin (Promega) in a volume of 50 mM NH_4HCO_3 sufficient to cover the gel pieces. Peptides were extracted from the gel pieces with 50% (v/v) ACN in 5% (v/v) FA and dried under a Centrivap concentrator (Labconco, Kansas City, MO, USA).

Phosphopeptide enrichment by TiO_2 affinity column chromatography

Phosphopeptides were enriched using the TitanspherePhospho-TiO Kit (GL Sciences, Tokyo, Japan) following the manufacturer's protocol. Briefly, the titanium dioxide (TiO_2) affinity column was conditioned with 20 μl of Buffer A (0.4% w/v TFA in 80% v/v ACN) by centrifuging twice at 3000 × g for 2 min and equilibrated with Buffer B (25% w/v lactic acid and 0.3% w/v TFA in 60% v/v ACN) by again centrifuging twice as before. The extracted peptides, which had been resuspended in 150 μl Buffer B, were loaded onto the column. For sample adsorption, the column was first centrifuged at 1000 × g for 10 min, and the flow-through was loaded onto the column and centrifuged again. The column was washed three times with 20 μl Buffer B by centrifugation at 3000 × g for 2 min, followed by washing with 20 μl Buffer A by centrifugation under the same conditions. Phosphorylated peptides were eluted twice with 50 μl 5% (v/v) NH_4OH and 50 μl 30% ACN by centrifugation at 1000 × g for 5 min. The eluate was evaporated in a Centrivap concentrator and stored at −20 °C until liquid chromatography-tandem mass spectrometry (LC-MS/MS) analysis.

Mass spectrometric analysis

Peptides were reconstituted in 2% (v/v) ACN in 0.4% (v/v) FA and separated on an in-house packed micro-capillary Michrom Magic C_{18} column (75 μm inner diameter, 12 cm length) by elution with a linear gradient of 2−32% Solvent B (0.1% v/v FA in ACN) in Solvent A (0.1% v/v FA in water) for 65 min at a flow rate of 300 nl min^{-1}. Samples were analyzed in triplicate on a Q-Exactive (Thermo Fisher Scientific, San Jose, CA, USA) hybrid quadrupole-Orbitrap mass spectrometry (MS), interfaced with a nano-ultra performance liquid chromatography system (Easy nLC, Thermo Fisher Scientific). The spray voltage was set to 2.0 kV, and the temperature of the heated capillary was set to 250 °C. The Q-Exactive was operated in data-dependent mode with one survey MS scan followed by 10 MS/MS scans and a dynamic exclusion time of 60 s. The full scans were acquired in the mass analyzer at 400 −1600 m/z with the resolution of 70 000, and the MS/MS scans were obtained with a resolution of 17 500 by using a normalized collision energy of 27% for high-energy collisional dissociation fragmentation. The automatic gain control target was 5e,[4] the maximum injection time was 120 ms and the isolation window was set to 3 m/z.

Database search and identification of the phosphoproteome

Collected raw files were converted into mzXML files through the Trans Proteomic Pipeline (version 4.5; Seattle Proteomic Center, Seattle, WA, USA). The peptides were assigned by the SEQUEST algorithm (Thermo Fisher Scientific, version 27, rev. 11) against the decoy IPI.HUMAN database (v.3.18, 120180 entries), and the false discovery rate (FDR) was estimated by Sorcerer (Sage-N Research, Milpitas, CA, USA). All searches were carried out based on trypsin specificity, allowing two missed cleavages. Carbamido-methylation of cysteine was set as fixed, and oxidation of methionine, phosphorylation of serine, threonine and tyrosine were set as variable modifications. The search considered a precursor ion mass tolerance of 10 p.p.m., and the fragment ion mass tolerance was set to 1.0 Da Scaffold (version 3.4.9; Proteome Software, Portland, OR) was used to compare spectral counts, validate MS/MS-based peptides and identify matching proteins according to the criteria of 99% minimum protein probability by the Protein Prophet algorithm,[18] with 80% minimum peptide probability and one minimum peptide (FDR <0.5%) as specified by the Peptide Prophet algorithm.[19] Proteins that contained redundant peptides and multiple isoforms, which could not be differentiated based on MS/MS spectra, were grouped into a primarily assigned protein. Scaffold PTM (version 1.1.3; Proteome Software) was used to annotate Post-Translational Modification (PTM) sites derived from MS/MS sequencing results. The Scaffold PTM assigned possible phosphorylation sites from the Scaffold validated tandem data using the Ascore algorithm developed by Beausoleil et al.[20]

Quantification and bioinformatic analysis of phosphoproteins

To quantify phosphoproteins, we used spectral counts of phospho-peptides from triplicate samples of SNU216 and SNU216-LR. The data set was entered into the R program (version 2.15) with power law global error model (PLGEM, version 1.28), a statistical analysis software package (www.bioconductor.org) used to determine signal-to-noise ratio and P-value.[21] Based on PLGEM, the annotation of protein cellular localization and evaluation of biological function was performed after uploading the signal-to-noise ratio and P-value to the Ingenuity Pathway Analysis (IPA; Ingenuity Systems; Redwood City, CA, USA) database content version 14197757. Hence, the phosphopeptides of the identified proteins, including those in proteins of the MET-mediated MAPK/ERK and PI3K/AKT signaling pathways, were manually quantified by the XCalibur program (Thermo Fisher Scientific). The quantification of precursor ion for the first isotopes of each ion was performed using the area of the peptides present in the raw data set across all samples in extracted ion chromatograms.

4

RESULTS

Identification of phosphoproteins in SNU216 and SNU216-LR cells

To investigate possible mechanisms responsible for acquiring resistance to HER2-targeted therapy in gastric cancer, we established a LR cell line (SNU216-LR) by chronically exposing HER2-positive SNU216 cells (lapatinib-hypersensitive gastric cancer cells) to increasing concentrations of lapatinib *in vitro* for 8 months. A LR cell clone (SNU216-LR) was selected and characterized. The half-maximal inhibitory concentration value in SNU216-LR cells was $> 10\,\mu\text{M}$, which is 500-fold higher than that of parental cells ($0.02\,\mu\text{M}$).

Next, we performed a large-scale quantitative phosphoproteome analysis to identify differentially phosphorylated proteins (DPPs) between SNU216-LR and SNU216 cells. A total of 6556 unique phosphopeptides representing 1686 phosphoproteins was identified with high confidence by MS analysis of the TiO_2-enriched phosphopeptides (protein: probability $> 99\%$ and FDR $< 1.5\%$; peptide: probability $> 80\%$ and FDR $< 0.5\%$), and 97.7% of proteins overlapped between SNU216 and SNU216-LR cell lines (Supplementary Figure 1A and Supplementary Tables 1 and 2). We then determined the phosphorylation sites of all identified phosphopeptides using Ascore and localization probability by Scaffold PTM.[20] Our approach identified 7791 phosphorylation sites (Ascore $> 80\%$) among 11 852 unique phosphorylation sites (Supplementary Table 3). Serine was found to be the most abundantly phosphorylated residue (9745 sites, 82%), followed by threonine (1763 sites, 15%) and tyrosine (344 sites, 3%) (Supplementary Figure 1B). The reproducibility of detecting the same proteins in triplicate analysis by LC-MS/MS exceeded 91% for both cell lines (Supplementary Figures 1C and 1D).

To estimate quantitative changes in the phosphorylation of each phosphopeptide, we selected DPPs in SNU216-LR cells using the spectral counting method in Scaffold (version 3.4.9). The signal-to-noise ratio and *P*-values for the DPPs were obtained using PLGEM. A list of 95 significantly regulated phosphoproteins ($P < 0.006$) is presented in Table 1. As shown in the volcano plot, 69 proteins were upregulated (red box), and 26 proteins were downregulated (blue box) in SNU216-LR cells (Figure 1a). To understand the functions of the DPPs, we examined cellular processes represented by the 95 regulated proteins using the IPA tool and found that they belong to enzyme (14%), transcription regulator (12%) and kinase (6%) groups of proteins (Figure 1b). We also examined the cellular distribution of these proteins and found that most were associated with either the nucleus (40%) or cytoplasm (35%), with fewer associated with the membrane (9%) (Figure 1c).

We further evaluated quantitative changes in phosphorylation of proteins using label-free quantification methods (MS/MS spectral count and extraction ion chromatography) that are generally accepted in phosphoproteomic studies.[22–24] More MS/MS spectral counts of phosphorylated EGFR and HER2 peptides were identified in SNU216-LR than SNU216 cells (Supplementary Figures 2A and 2B). These data were consistent with the peptide extracted ion chromatogram, which showed significantly greater signal intensities of phosphorylated peptides in SNU216-LR cells (Supplementary Figures 2C and 2D). Using the same quantification approaches, we were able to measure the phosphorylation levels of key molecules (MET, RAS, C-RAF, ERK1/2, PI3K and AKT; see Supplementary Figures 2E–J). In addition, we found a new phosphorylation site in HER2 (S1073) based on the phosphopeptide reference database phosphoSitePlus (www.phosphosite.org). This phosphorylation site was confirmed by the matched tandem mass spectra shown in Supplementary Figure 3.

Network analysis and quantification of differentially phosphorylated proteins

To investigate the extent to which activation of signaling pathways contributes to EGFR/HER2-targted therapy, we integrated the DPPs ($P < 0.006$) into the protein interaction network using the IPA tool to interpret the DPPs in the context of biological processes. The IPA tool generated the top three networks that are associated with cancer, cell morphology and cellular and tissue development (Supplementary Figure 4). Considering this network analysis, our upregulated phosphoproteins, including EGFR and MET, appeared to be closely related to PI3K, AKT and ERK1/2 in SNU 216-LR (Figure 2).

Our analysis of results from the IPA tool also revealed that EGFR/HER2, MET and ERK/MAPK signaling pathways were enriched (Supplementary Figure 5). Based on the results from the network and canonical signaling pathway analyses, we constructed the signaling network for EGFR/HER2 and MET with the two major downstream signaling pathways (PI3K/AKT and MAPK/ERK) including SRC (Figure 3). As shown in Figure 3a, categorization of expression levels of specific phosphorylated sites revealed that the majority of signaling molecules were highly expressed in SNU216-LR. We further compared SNU216 and SNU216 LR, as well as three other resistant clones (SNU216-LR1, 2 and 3), using immunoblot analysis with phospho-specific antibodies. Consistent with the quantitative MS results, the phosphorylation level of selected proteins (EGFR, HER2, MET, AKT, MAPK, SRC, and RAF) was increased in SNU216-LR (Figure 3b).

Effects of targeted anticancer agents on SNU216-LR cells

To verify whether constitutive activation of the PI3K/AKT and MAPK/ERK signaling pathways is the MET-mediated cascade that confers an acquired lapatinib resistance, we investigated the effects of selected kinase inhibitors, including lapatinib, NVP-BEZ235 (PI3K/mTOR inhibitor), selumetinib (MEK inhibitor), saracatinib (SRC inhibitor) and crizotinib (MET inhibitor), on the growth of SNU216-LR cells. As shown in Figure 4a, combination treatment with these drugs had a greater inhibitory effect on cell growth in SNU216-LR cells compared with single-agent treatment. The combination of lapatinib and NVP-BEZ235 produced the best growth inhibition effect. To confirm our data, we investigated cell cycle

Table 1 Differentially expressed phosphoproteins in SNU216-LR ($P < 0.006$)

ID	Protein	Symbol	Location	Type(s)	S/N	P-value
IPI00292009	Palladin	PALLD	Cytoplasm	Other	6.09	0.00000
IPI00555610	313 kDa protein	—	—	—	4.97	0.00000
IPI00657687	Isoform 1 of Actin-binding protein anillin	ANLN	Cytoplasm	Other	4.60	0.00000
IPI00008868	Microtubule-associated protein 1B	MAP1B	Cytoplasm	Other	3.61	0.00002
IPI00008918	Isoform β of LIM domain and actin-binding protein 1	LIMA1	Cytoplasm	Other	3.61	0.00004
IPI00291802	Isoform 3 of LIM domain only protein 7	LMO7	Cytoplasm	Enzyme	3.42	0.00005
IPI00304589	182 kDa tankyrase 1-binding protein	TNKS1BP1	Nucleus	Other	3.10	0.00008
IPI00029273	Isoform 1 of Hepatocyte growth factor receptor precursor	MET	Plasma membrane	Kinase	3.01	0.00010
IPI00009286	Isoform 1 of zinc finger protein HRX	MLL	Nucleus	Transcription regulator	2.96	0.00010
IPI00219301	Myristoylated alanine-rich C-kinase substrate	MARCKS	Plasma membrane	Other	2.90	0.00014
IPI00745518	Microtubule-associated protein 4 isoform 1 variant (Fragment)	—	—	—	2.88	0.00018
IPI00013076	Isoform 1 of FGFR1 oncogene partner	FGFR1OP	Cytoplasm	Other	2.77	0.00021
IPI00028481	Ras-related protein Rab-8A	RAB8A	Plasma membrane	Other	2.68	0.00026
IPI00006196	Isoform 2 of Nuclear mitotic apparatus protein 1	NUMA1	Nucleus	Other	2.65	0.00028
IPI00329115	Isoform 1 of protein C10orf47	C10orf47	Unknown	Other	2.57	0.00030
IPI00289334	Isoform 1 of filamin-B	FLNB	Cytoplasm	Other	2.55	0.00030
IPI00658152	Tensin-like SH2 domain containing 1	TNS3	Unknown	Phosphatase	2.54	0.00030
IPI00237884	Isoform 1 of A-kinase anchor protein 12	AKAP12	Cytoplasm	Transporter	2.51	0.00046
IPI00216219	Isoform long of tight junction protein ZO-1	TJP1 (includes EG:21872)	Plasma membrane	Other	2.48	0.00046
IPI00218753	Isoform 3 of DNA topoisomerase 2-α	TOP2A	Nucleus	Enzyme	2.47	0.00046
IPI00294742	HDCMA18P protein	LARP7	Unknown	Other	2.45	0.00047
IPI00020513	Zyxin	ZYX	Plasma membrane	Other	2.36	0.00060
IPI00298289	Isoform 2 of reticulon-4	RTN4	Cytoplasm	Other	2.27	0.00068
IPI00157144	GYS1 protein	GYS1	Cytoplasm	Enzyme	2.21	0.00076
IPI00010471	Plastin-2	LCP1	Cytoplasm	Other	2.20	0.00078
IPI00178440	Elongation factor 1-β	EEF1B2	Cytoplasm	Translation regulator	2.18	0.00078
IPI00220740	Isoform 2 of nucleophosmin	NPM1	Nucleus	Transcription regulator	2.16	0.00081
IPI00552897	Isoform 1 of mediator of DNA damage checkpoint protein 1	MDC1	Nucleus	Other	2.16	0.00083
IPI00294840	Absent in melanoma 1 protein	AIM1 (includes EG:11630)	Unknown	Other	2.15	0.00084
IPI00031605	AHNAK nucleoprotein, isoform 2	AHNAK	Nucleus	Other	2.12	0.00098
IPI00015029	Prostaglandin E synthase 3	PTGES3	Cytoplasm	Enzyme	2.11	0.00099
IPI00032064	Isoform A of A-kinase anchor protein 2	—	—	—	2.10	0.00099
IPI00152011	PTPL1-associated RhoGAP 1	ARHGAP29	Cytoplasm	Other	2.10	0.00101
IPI00015953	Isoform 1 of nucleolar RNA helicase 2	DDX21	Nucleus	Enzyme	2.09	0.00101
IPI00004233	Isoform long of antigen KI-67	MKI67	Nucleus	Other	2.08	0.00103
IPI00027831	Glutamate-rich WD repeat-containing protein 1	GRWD1	Nucleus	Other	2.02	0.00111
IPI0419933	Pleckstrin homology domain containing, family A member 2	PLEKHA7	Cytoplasm	Other	2.02	0.00111
IPI00017450	Transcription initiation factor IIF α subunit	GTF2F1	Nucleus	Transcription regulator	2.01	0.00132
IPI00219841	DNA ligase 1	LIG1	Nucleus	Enzyme	1.97	0.00144
IPI00218136	137 kDa protein	CGN	Plasma Membrane	Other	1.95	0.00149

Table 1 (Continued)

ID	Protein	Symbol	Location	Type(s)	S/N	P-value
IPI00020021	Protein DEK	DEK	nucleus	Transcription regulator	1.92	0.00161
IPI00031698	Hypothetical protein MGC5509	C2orf49	Unknown	Other	1.90	0.00177
IPI00033054	CTD small phosphatase like 2	CTDSPL2	Unknown	Other	1.89	0.00179
IPI00376199	Interferon regulatory factor 2 binding protein 2	IRF2BP2	Nucleus	Transcription regulator	1.85	0.00195
IPI00411635	KIAA0802 protein	—	—	—	1.83	0.00202
IPI00005688	Zinc finger protein 185	ZNF185	Nucleus	Other	1.82	0.00206
IPI00470483	WD repeat domain 62	WDR62	Nucleus	Other	1.77	0.00219
IPI00152881	Shroom-related protein	SHROOM3	Cytoplasm	Other	1.76	0.00225
IPI00337426	Isoform 1 of BMP-2-inducible protein kinase	BMP2K	Nucleus	Kinase	1.76	0.00225
IPI00025512	Heat-shock protein β-1	HSPB1	Cytoplasm	Other	1.73	0.00265
IPI00456887	Scaffold attachment factor A2	HNRNPUL2	Nucleus	Other	1.71	0.00272
IPI00020418	Ras-related protein R-Ras	RRAS	Cytoplasm	Enzyme	1.70	0.00277
IPI00291175	Isoform 1 of vinculin	VCL	Plasma membrane	Enzyme	1.66	0.00291
IPI00010746	Phosphatidylserine synthase 1	PTDSS1	Cytoplasm	Enzyme	1.61	0.00336
IPI00216654	Isoform β of nucleolar phosphoprotein p130	NOLC1	Nucleus	Transcription regulator	1.59	0.00365
IPI00645814	KIAA1187 protein	MAP7D1	Unknown	Other	1.58	0.00370
IPI00019996	modulator of estrogen induced transcription isoform b	SLTM	Nucleus	Other	1.56	0.00388
IPI00013743	Hypothetical protein BUD13	BUD13 (includes EG:215051)	Nucleus	Other	1.54	0.00400
IPI00024579	Postreplication repair protein RAD18	RAD18	Nucleus	Other	1.52	0.00406
IPI00025087	Isoform 1 of Cellular tumor antigen p53	TP53 (includes EG:22059)	Nucleus	Transcription regulator	1.52	0.00406
IPI00008708	Ribosomal L1 domain-containing protein 1	RSL1D1	Cytoplasm	Other	1.51	0.00448
IPI00295457	Myosin phosphatase-Rho interacting protein isoform 1	MPRIP	Cytoplasm	Other	1.50	0.00449
IPI00002135	Transforming acidic coiled-coil-containing protein 3	TACC3	Nucleus	Other	1.49	0.00458
IPI00184317	Isoform short of transcription intermediary factor 1-α	TRIM24	Nucleus	Transcription regulator	1.49	0.00508
IPI00394829	Hypothetical protein LOC286077	FAM83H	Unknown	Other	1.48	0.00512
IPI00294618	Proline-rich protein PRCC	PRCC	Nucleus	Other	1.45	0.00534
IPI00181905	Isoform 1 of protein KIAA1914	AFAP1L2	Cytoplasm	Other	1.44	0.00560
IPI00302829	Retinoblastoma-associated protein	RB1	Nucleus	Transcription regulator	1.43	0.00569
IPI00018274	Isoform 1 of epidermal growth factor receptor precursor	EGFR	Plasma membrane	Kinase	1.40	0.00598
IPI00289819	Cation-independent mannose-6-phosphate receptor precursor	IGF2R	Plasma membrane	Transmembrane receptor	−1.39	0.00592
IPI00019870	Isoform α of caveolin-2	CAV2	Plasma membrane	Other	−1.43	0.00543
IPI00301294	Protein C2orf17	FAM134A	Unknown	Other	−1.43	0.00543
IPI00100151	5′–3′ exoribonuclease 2	XRN2	Nucleus	Enzyme	−1.44	0.00528
IPI00010080	Serine/threonine-protein kinase OSR1	OXSR1	Nucleus	Kinase	−1.45	0.00520
IPI00719818	Nucleolar protein 5A	NOP56	Nucleus	Other	−1.46	0.00496
IPI00011635	Isoform 2 of Bcl-2-like 13 protein	BCL2L13	Cytoplasm	Other	−1.47	0.00482
IPI00006987	ATP-dependent RNA helicase DDX24	DDX24	Nucleus	Enzyme	−1.49	0.00474
IPI00032107	Sulfate transporter	SLC26A2	Plasma membrane	Transporter	−1.49	0.00465

Table 1 (Continued)

ID	Protein	Symbol	Location	Type(s)	S/N	P-value
IPI00297859	Isoform 1 of myeloid/lymphoid or mixed-lineage leukemia protein 2	MLL2	Nucleus	Transcription regulator	−1.49	0.00465
IPI00019502	Myosin-9	MYH9	Cytoplasm	Enzyme	−1.54	0.00377
IPI00004273	RNA binding motif protein 25	RBM25	Nucleus	Other	−1.54	0.00377
IPI00009146	FLN29 gene product	TRAFD1	Unknown	Other	−1.62	0.00291
IPI00719759	Akt substrate AS250	RALGAPA2	Cytoplasm	Other	−1.62	0.00291
IPI00396634	OTTHUMP00000028561	KIAA1671	Unknown	Other	−1.65	0.00274
IPI00217709	Isoform β-1 of DNA topoisomerase 2-β	TOP2B	Nucleus	Enzyme	−1.72	0.00251
IPI00025156	Isoform 1 of STIP1 homology and U box-containing protein 1	STUB1	Cytoplasm	Enzyme	−1.84	0.00180
IPI00554788	Keratin, type I cytoskeletal 18	KRT18	Cytoplasm	Other	−1.84	0.00179
IPI00061758	PRR8 protein	RBM33	Unknown	Other	−1.89	0.00168
IPI00304587	Dispatched B	DISP2	Unknown	Other	−2.02	0.00120
IPI00021275	Isoform 1 of ephrin type-B receptor 2 precursor	EPHB2	Plasma membrane	Kinase	−2.33	0.00063
IPI00024062	Band 4.1-like protein 1	EPB41L1	Plasma membrane	Other	−2.49	0.00044
IPI00744036	Tight junction protein 3	TJP3	Plasma membrane	Other	−3.04	0.00007
IPI00748920	Splicing coactivator subunit SRm300	SRRM2	Nucleus	Other	−3.40	0.00004
IPI00304875	Isoform 1 of HIRA-interacting protein 3	HIRIP3	Nucleus	Other	−3.62	0.00002
IPI00395887	Thioredoxin domain-containing protein 1 precursor	TMX1	Cytoplasm	Enzyme	−5.34	0.00000

Abbreviation: S/N, signal-to-noise ratio.
Up- or down-regulated phosphoproteins in SNU216-LR compared with SNU216 cells. S/N and P-values were generated by the power law global error model (PLGEM) statistical analysis tool.
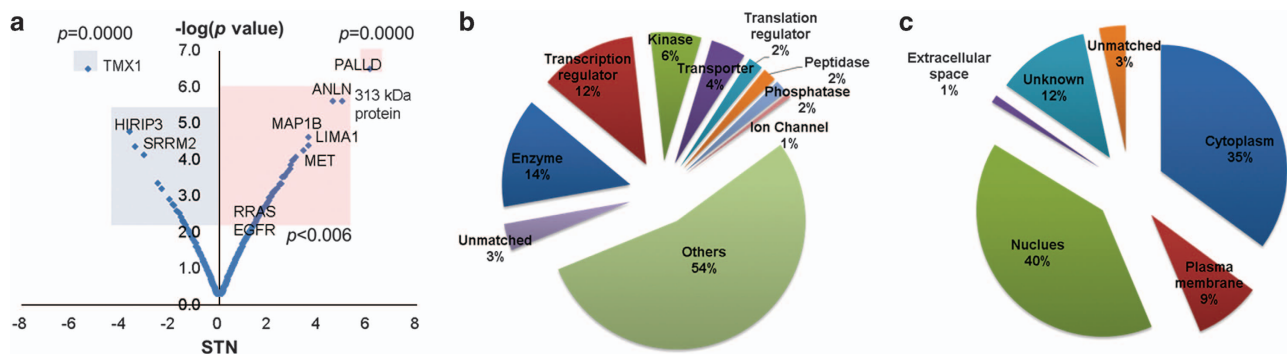

Figure 1 Differentially expressed phosphoproteins in SNU216-LR and their functional annotations. (**a**) Volcano plot showing the P-value ($-\log_{10}$) versus signal-to-noise ratio (S/N) of phosphoproteins determined by power law global error model (PLGEM) statistical analysis for label-free quantification. (**b**) Molecular functions of identified phosphoproteins by the Ingenuity Pathway Analysis (IPA) tool. (**c**) Subcellular localization of identified phosphoproteins by the IPA tool.

arrest by staining the cells with the DNA-intercalating dye propidium iodide. Combination treatment with lapatinib and NVP-BEZ235, selumetinib, saracatinib or crizotinib induced an increase in the percentage of SNU216-LR cells in the G1 phase compared with single-agent treatment (Figure 4b). Next, we examined the levels of total and phosphorylated EGFR, HER2, MET, AKT, MAPK, SRC, cyclin D and p27 in SNU216-LR cells (Figure 4c). As expected, treatment with NVP-BEZ235, selumetinib, sacaratinib or crizotinib alone reduced the phosphorylation level of each target or of the downstream

effectors (AKT, MAPK, SRC and MET, respectively). The phosphorylation levels of the selected signaling molecules remained the same after treatment with dimethyl sulfoxide (control) or lapatinib. Treatment with a single kinase inhibitor had no effect on the expression of cell cycle regulatory molecules, including cyclin D. The combination treatment of lapatinib with a kinase inhibitor showed markedly decreased phosphorylation levels in each of the target molecules, such as EGFR and HER2, as well as in the downstream effectors, compared with single treatment. Furthermore, the levels of cell
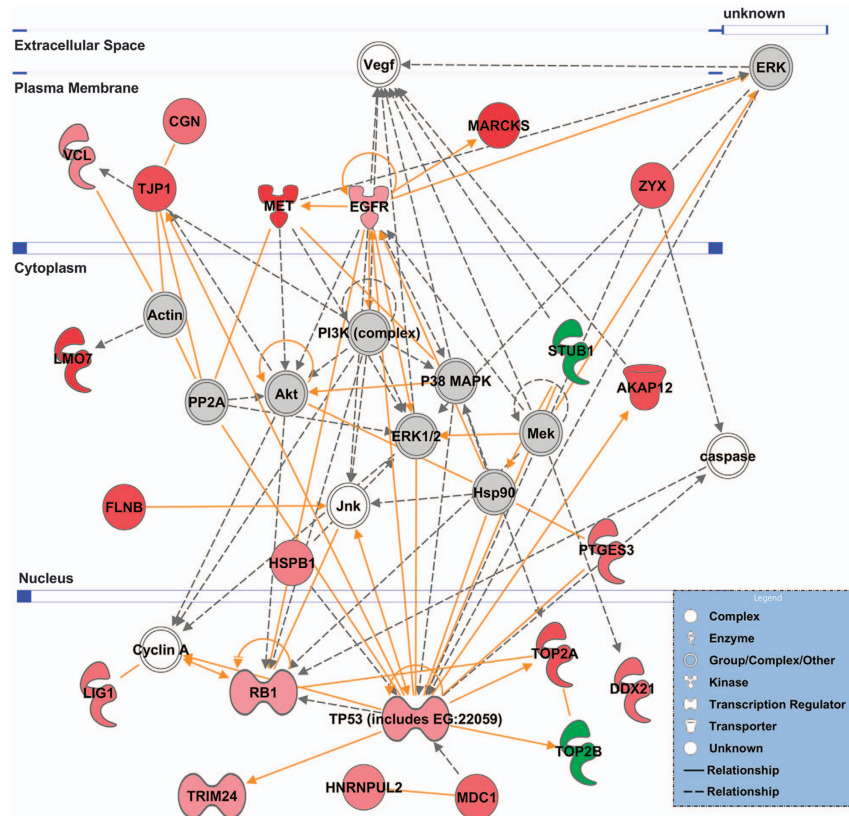
Figure 2 Biological network analysis of phosphoproteins. Associations among phosphoproteins are shown by solid or dashed lines, which represent direct or indirect interactions, respectively. Upregulated proteins are shown in red, and downregulated proteins are shown in green.

proliferation-related cyclin D were reduced, and those of the cell cycle inhibitor p27 were increased, after combination treatment. The levels of p-SRC in SNU216-LR were not affected by individual TKI treatment or the combination treatment except the SRC inhibitor (saracatinib) when p-SRC was monitored with the specific tyrosine antibody (Y416). As SRC is known to be an essential communicator between EGFR and MET in LR cancer cells,[25] maintaining SRC activation may be necessary for efficient compensatory TKI activation for acquired TKI resistance.

DISCUSSION

Lapatinib inhibits growth of HER2-positive gastric cancer cell lines.[9] Presently, a phase III clinical trial in patients with advanced gastric cancer is on-going, studying the effects of lapatinib in combination with capecitabine plus oxaliplatin.[26] Interest in this trial reflects lapatinib being regarded as one of the promising chemotherapeutic drugs for gastric cancer treatment. On the other hand, the medium duration of response to lapatinib is <1 year, and almost 80% of trastuzumab-pretreated patients fail to respond to lapatinib.[27] Hence, understanding the mechanisms of acquired lapatinib resistance may help to improve the therapeutic efficacy of lapatinib in HER2-positive cancers.

To identify molecular changes conferring resistance to lapatinib at the system level, we performed a quantitative

phosphoprotein profiling of the isogenic gastric cancer cell lines SNU216-LR and SNU216, in which we identified a total of 11 852 phosphorylation sites on 1686 phosphoproteins. Integrating the DPPs into cellular signaling pathways using the IPA network analysis tool provided potential signaling pathways that are regulated in response to lapatinib-induced resistance in SNU216-LR. Among the predominant signaling pathways generated from the IPA analysis, we highlighted the following: three receptor tyrosine kinases (EGFR, HER2 and MET); the two major downstream signaling pathways (PI3K/ AKT and MAPK/ERK); and SRC. We found that the PI3K/ AKT and MAPK/ERK signaling pathways and SRC were constitutively activated in SNU216-LR cells. This observation is similar to those of Rexer *et al.*,[28] who observed active PI3K/AKT and MAPK pathways, including increased phosphorylation of SRC, in LR HER2-overexpressing human breast cancer cells. Activation of the SRC pathway is essential for communication between EGFR and MET.[25] For example, lateral signaling in the EGFR/SRC/MET axis was indicated by a delay in the EGFR activation of MET in non-small-cell lung cancer produced by an inhibitor of SRC. Interestingly, our data in SNU216-LR cells show a similar pattern of lateral activation of EGFR/SRC/MET, suggesting that cross-talk between EGFR and MET may play a significant role in the regulation of SNU216-LR cells. Our conclusions are also supported by the fact that functional cross-talk between EGFR and MET has
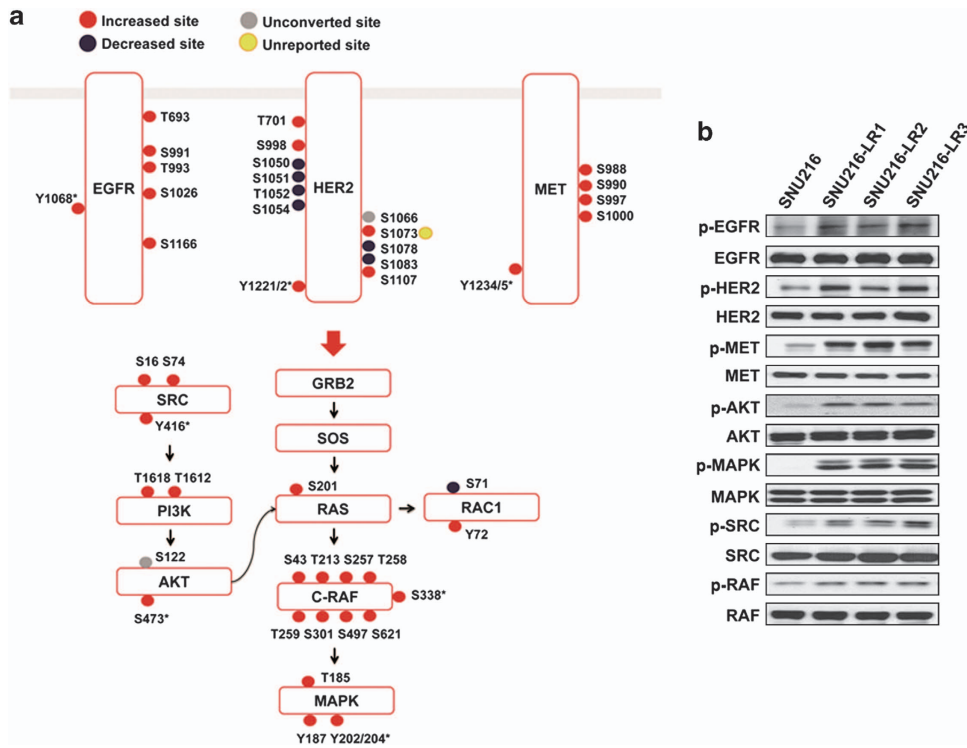
Figure 3 Merged signaling pathways in SNU216-LR. (**a**) Reconstructed EGFR/HER2 and MET signaling pathways with two downstream signaling pathways (PI3K/AKT and MAPK/ERK). Red, blue and yellow closed circles on each protein represent increased, decreased and newly identified phosphorylation sites in SNU216-LR, respectively. Specific phosphorylated sites (marked with an asterisk) of HER2, EGFR, MET, SRC, C-RAF and MAPK were also identified from immunoblot analysis with antibodies against p-EGFR (pY1068), p-HER2 (pY1221/1222), p-MET (pY1234/1235), p-AKT (pS473), p-MAPK (pY202/pY204), p-SRC (pY416) and p-RAF (pS338). Protein names for symbols are as follows: AKT, α-serine/threonine-protein kinase; C-RAF, RAF proto-oncogene serine/threonine-protein kinase; EGFR, epidermal growth factor receptor; ERK, extracellular signal-regulated kinase; HER2, human epidermal growth factor receptor 2; MAPK, mitogen-activated protein kinase 1; GRB2, growth factor receptor-bound protein 2; MET, hepatocyte growth factor/mesenchymal–epithelial transition factor; PI3K, phosphatidylinositide 3-kinase; RAC1, Ras-related C3 botulinum toxin substrate 1; RAS, Ras-related protein R-Ras; SOS, son of sevenless homolog; SRC, proto-oncogene tyrosine protein kinase Src. (**b**) Immunoblot analysis of SNU216 and three different resistant clones (SNU216-LR 1, 2 and 3) with phospho-tyrosine or serine-specific antibodies. α-Tubulin was used as a loading control. Data are representative of three independent experiments.

been extensively documented as playing an important role in drug resistance. Engelman *et al.*[14] have demonstrated that the compensatory activation of MET is responsible for resistance to EGFR-targeting drugs.[14] Puri *et al.*[29] also observed that inhibition of MET in non-small-cell lung cancer is synergistic with EGFR inhibition.

Having found the constitutive activation in LR gastric cancer cells of the PI3K/AKT and MAPK/ERK signaling pathways, as well as activation of SRC, we hypothesized that the constitutive activation of PI3K/AKT and MAPK/ERK confers resistance to lapatinib and may be mediated by MET-axis signaling along the two major downstream pathways. Our data are consistent with the notion of compensatory activation of MET-mediated downstream cellular signaling pathway in response to EGFR blockade.[30,31] Results from several studies have indicated that MET activation is associated with both primary and acquired resistance to EGFR inhibitors in non-small-cell lung cancer.[14,15,32,33] Therefore, we postulate that constitutive activation of the MET-axis PI3K/AKT and MAPK/ERK signaling pathways, including the lateral

activation of SRC, is a compensatory signaling cascade counteracting the selective pressure on EGFR/HER2 in LR human gastric cancer cells.

In the present study, we found that cotreatment with lapatinib and crizotinib is able to induce lapatinib sensitivity. Thus, the active PI3K/AKT and MAPK/ERK signaling pathways induced by the MET axis may be a critical compensatory intracellular event for the survival of LR cells.[28] To the best of our knowledge, the present study is the first large-scale profiling of peptide/protein phosphorylation in gastric cancer cell lines to study lapatinib resistance. Our site-specific and semiquantitative approach demonstrates a useful bioinformatics application, and phosphoproteomic data from the study provide information directly relevant to the mechanisms of lapatinib resistance.

In conclusion, we demonstrated that network-based global phosphoproteomic analysis is a reliable approach for predicting cellular signaling events in LR gastric cancer cells. Our results suggest that the MET-directed PI3K/AKT and MAPK/ERK cellular signaling pathways contribute to lapatinib
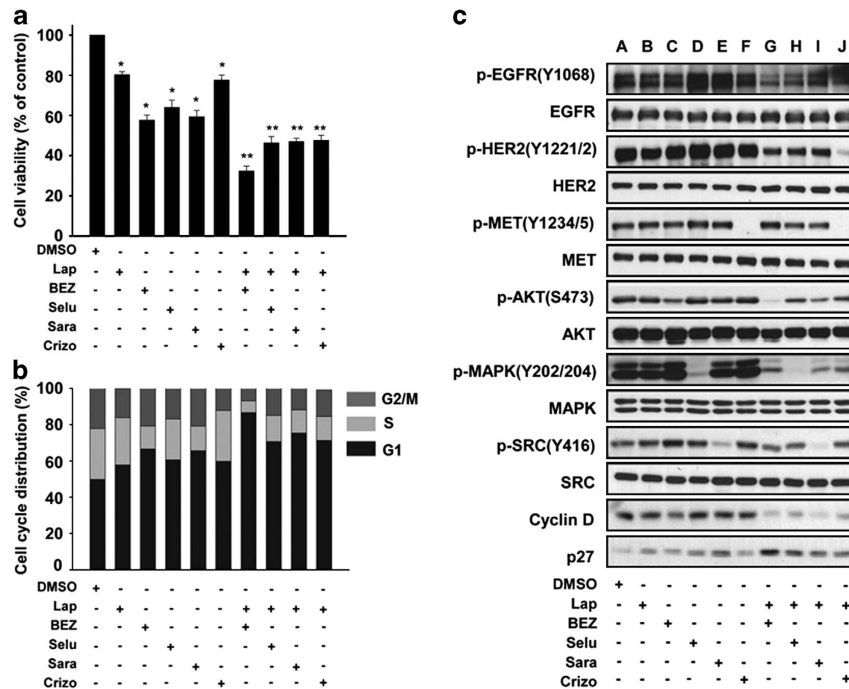
Figure 4 Antiproliferative effects of selected tyrosine kinase inhibitors on SNU216-LR. SNU216-LR cells were treated via single or combined treatment of lapatinib (Lap; 1 μM), NVP-BEZ235 (BEZ; 100 nM), selumetinib (Selu; 1 μM), saracatinib (Sara; 1 μM) and crizotinib (Crizo; 1 μM). (a) Viable cells were measured after 72 h. The percentage of viable cells is shown relative to untreated controls. Data represent the mean ± s.d. (*P < 0.05 for single vs dimethyl sulfoxide (DMSO); **P < 0.05 for combination vs single) from three independent experiments. (b) Cells were fixed with 70% (v/v) ethanol, stained with propidium iodide and analyzed using flow cytometry. The proportion of cells in the G1, S and G2/M phases were quantified using the ModFit LT program (Verity Software House). Columns represent the means of three independent experiments. (c) SNU216-LR cells were treated with the indicated drug for 48 h. Whole-cell extracts were analyzed by western blot with antibodies recognizing phosphorylated and total EGFR, HER2, MET, AKT, MAPK, SRC, cyclin D and p27. Data are representative of three independent experiments. AKT, α-serine/threonine-protein kinase; EGFR, epidermal growth factor receptor; HER2, human epidermal growth factor receptor 2; MAPK, mitogen-activated protein kinase 1; MET, hepatocyte growth factor/mesenchymal–epithelial transition factor; SRC, proto-oncogene tyrosine protein kinase Src.

resistance, and the constituent signaling molecules may be potential targets for the development of complementary therapeutic options. Therefore, the validity of MET-axis PI3K/AKT and MAPK/ERK signaling pathways should be evaluated using clinical samples and will be the subject of further investigations.

CONFLICT OF INTEREST
The authors declare no conflict of interest.

1 Monsey J, Shen W, Schlesinger P, Bose R. Her4 and Her2/neu tyrosine kinase domains dimerize and activate in a reconstituted *in vitro* system. *J Biol Chem* 2010; **285**: 7035–7044.

2 Higa GM, Abraham J. Lapatinib in the treatment of breast cancer. *Expert Rev Anticancer Ther* 2007; **7**: 1183–1192.

3 Slamon DJ, Clark GM, Wong SG, Levin WJ, Ullrich A, McGuire WL. Human breast cancer: correlation of relapse and survival with amplification of the HER-2/neu oncogene. *Science* 1987; **235**: 177–182.

4 Slamon DJ, Godolphin W, Jones LA, Holt JA, Wong SG, Keith DE et al. Studies of the HER-2/neu proto-oncogene in human breast and ovarian cancer. *Science* 1989; **244**: 707–712.

5 De Vita F, Giuliani F, Silvestris N, Catalano G, Ciardiello F, Orditura M. Human epidermal growth factor receptor 2 (HER2) in gastric cancer: a new therapeutic target. *Cancer Treat Rev* 2010; **36** (Suppl 3), S11–S15.

6 Rusnak DW, Lackey K, Affleck K, Wood ER, Alligood KJ, Rhodes N et al. The effects of the novel, reversible epidermal growth factor receptor/ErbB-2 tyrosine kinase inhibitor, GW2016, on the growth of human normal and tumor-derived cell lines in vitro and in vivo. *Mol Cancer Ther* 2001; **1**: 85–94.

7 Cameron DA, Stein S. Drug insight: intracellular inhibitors of HER2–clinical development of lapatinib in breast cancer. Nature clinical practice. *Oncology* 2008; **5**: 512–520.

8 Ryan Q, Ibrahim A, Cohen MH, Johnson J, Ko CW, Sridhara R et al. FDA drug approval summary: lapatinib in combination with capecitabine for previously treated metastatic breast cancer that overexpresses HER-2. *Oncologist* 2008; **13**: 1114–1119.

9 Kim JW, Kim HP, Im SA, Kang S, Hur HS, Yoon YK et al. The growth inhibitory effect of lapatinib, a dual inhibitor of EGFR and HER2 tyrosine kinase, in gastric cancer cell lines. *Cancer Lett* 2008; **272**: 296–306.

10 Kim HP, Yoon YK, Kim JW, Han SW, Hur HS, Park J et al. Lapatinib, a dual EGFR and HER2 tyrosine kinase inhibitor, downregulates thymidylate synthase by inhibiting the nuclear translocation of EGFR and HER2. *PLoS One* 2009; **4**: e5933.

11 GlaxoSmithKline. Lapatinib optimization study in ErbB2 (HER2) positive gastric cancer: a phase III global, blinded study designed to evaluate clinical endpoints and safety of chemotherapy plus lapatinib http://clinicaltrials.gov/ct2/show/NCT00680901 2008

12 Nahta R, Yuan LXH, Du Y, Esteva FJ. Lapatinib induces apoptosis in trastuzumab-resistant breast cancer cells: effects on insulin-like growth factor I signaling. *Mol Cancer Ther* 2007; **6:** 667–674.

13 Chen FL, Xia W, Spector NL. Acquired resistance to small molecule ErbB2 tyrosine kinase inhibitors. *Clin Cancer Res* 2008; **14:** 6730–6734.

14 Engelman JA, Zejnullahu K, Mitsudomi T, Song Y, Hyland C, Park JO *et al.* MET amplification leads to gefitinib resistance in lung cancer by activating ERBB3 signaling. *Science* 2007; **316:** 1039–1043.

15 Yano S, Wang W, Li Q, Matsumoto K, Sakurama H, Nakamura T *et al.* Hepatocyte growth factor induces gefitinib resistance of lung adenocarcinoma with epidermal growth factor receptor-activating mutations. *Cancer Res* 2008; **68:** 9479–9487.

16 Chen CT, Kim H, Liska D, Gao S, Christensen JG, Weiser MR. Met activation mediates resistance to lapatinib inhibition of HER2-amplified gastric cancer cells. *Mol Cancer Ther* 2012; **11:** 660–669.

17 Rosenfeld J, Capdevielle J, Guillemot JC, Ferrara P. In-gel digestion of proteins for internal sequence analysis after one-or two-dimensional gel electrophoresis. *Anal Biochem* 1992; **203:** 173–179.

18 Nesvizhskii AI, Keller A, Kolker E, Aebersold R. A statistical model for identifying proteins by tandem mass spectrometry. *Anal Chem* 2003; **75:** 4646–4658.

19 Keller A, Nesvizhskii AI, Kolker E, Aebersold R. Empirical statistical model to estimate the accuracy of peptide identifications made by MS/MS and database search. *Anal Chem* 2002; **74:** 5383–5392.

20 Beausoleil SA, Villen J, Gerber SA, Rush J, Gygi SP. A probability-based approach for high-throughput protein phosphorylation analysis and site localization. *Nat Biotechnol* 2006; **24:** 1285–1292.

21 Lee YY, McKinney KQ, Ghosh S, Iannitti DA, Martinie JB, Caballes FR *et al.* Subcellular tissue proteomics of hepatocellular carcinoma for molecular signature discovery. *J Proteome Res* 2011; **10:** 5070–5083.

22 Mayya V, Lundgren DH, Hwang SI, Rezaul K, Wu L, Eng JK *et al.* Quantitative phosphoproteomic analysis of T cell receptor signaling reveals system-wide modulation of protein-protein interactions. *Sci Signal* 2009; **2ra46.**

23 Casado P, Cutillas PR. A self-validating quantitative mass spectrometry method for assessing the accuracy of high-content phosphoproteomic experiments. *Mol Cell Proteomics* 2011; **10:** M110 003079.

24 Alcolea MP, Casado P, Rodriguez-Prados JC, Vanhaesebroeck B, Cutillas PR. Phosphoproteomic analysis of leukemia cells under basal and drug-treated conditions identifies markers of kinase pathway activation and mechanisms of resistance. *Mol Cell Proteomics* 2012; **11:** 453–466.

25 Dulak AM, Gubish CT, Stabile LP, Henry C, Siegfried JM. HGF-independent potentiation of EGFR action by c-Met. *Oncogene* 2011; **30:** 3625–3635.

26 Kulig J, Kolodziejczyk P, Kulig P, Legutko J. Targeted therapy for gastric cancer–current status. *J Oncol Pharm Pract* 2013; **19:** 75–81.

27 Nahta R, Shabaya S, Ozbay T, Rowe DL. Personalizing HER2-targeted therapy in metastatic breast cancer beyond HER2 status: what we have learned from clinical specimens. *Curr Pharmacogenomics Person Med* 2009; **7:** 263–274.

28 Rexer BN, Ham AJ, Rinehart C, Hill S, Granja-Ingram Nde M, Gonzalez-Angulo AM *et al.* Phosphoproteomic mass spectrometry profiling links Src family kinases to escape from HER2 tyrosine kinase inhibition. *Oncogene* 2011; **30:** 4163–4174.

29 Puri N, Salgia R. Synergism of EGFR and c-Met pathways, cross-talk and inhibition, in non-small cell lung cancer. *J Carcinog* 2008; **7:** 9.

30 Xu H, Stabile LP, Gubish CT, Gooding WE, Grandis JR, Siegfried JM. Dual blockade of EGFR and c-Met abrogates redundant signaling and proliferation in head and neck carcinoma cells. *Clin Cancer Res* 2011; **17:** 4425–4438.

31 Stabile LP, Rothstein ME, Keohavong P, Lenzner D, Land SR, Gaither-Davis AL *et al.* Targeting of both the c-Met and EGFR pathways results in additive inhibition of lung tumorigenesis in transgenic mice. *Cancers* 2010; **2:** 2153–2170.

32 Agarwal S, Zerillo C, Kolmakova J, Christensen JG, Harris LN, Rimm DL *et al.* Association of constitutively activated hepatocyte growth factor receptor (Met) with resistance to a dual EGFR/Her2 inhibitor in non-small-cell lung cancer cells. *Br J Cancer* 2009; **100:** 941–949.

33 McDermott U, Pusapati RV, Christensen JG, Gray NS, Settleman J. Acquired resistance of non-small cell lung cancer cells to MET kinase inhibition is mediated by a switch to epidermal growth factor receptor dependency. *Cancer Res* 2010; **70:** 1625–1634.

Supplementary Information accompanies the paper on Experimental & Molecular Medicine website (http://www.nature.com/emm)